

**INHIBITION OF CHOLINE KINASE AS AN  
ANTIAMOEBIAC APPROACH IN *ENTAMOEBIA*  
*HISTOLYTICA***

**TEH ZHI HUI**

**UNIVERSITI SAINS MALAYSIA**

**2018**

**INHIBITION OF CHOLINE KINASE AS AN  
ANTIAMOEBIAC APPROACH IN *ENTAMOEBIA*  
*HISTOLYTICA***

**By**

**TEH ZHI HUI**

**Thesis submitted in fulfilment of the requirements**

**for the degree of**

**Master of Science**

**April 2018**

## **ACKNOWLEDGEMENT**

I am deeply indebted to my supervisors and teachers, Associate Professor Dr. Few Ling Ling, Associate Professor Dr. See Too Wei Cun, and Associate Professor Dr. Lim Boon Huat for their expert guidance, support, tolerance, and patience throughout this study. My utmost appreciation to USM Fellowship and Grant no. 1001/PPSK/812179, for the financial assistance provided.

My master's degree journey would not have been possible without constant love and encouragement from Chong Seok Im, Teh Sin Boey, Zhi Ying, and Zhi Khan. Special thanks to Pearl Cheah and Shobana Gunasegaran for the inspiration and motivation throughout these years.

A huge thanks to all my supportive friends, Dr. Wong Weng Kin, Dr. Foo Phiaw Chong, Dr Kang In Nee, Nurul Aini, Norhazilah, Nurul Fatihah, Goh Wei Chiang, Sharzehan, Anisah Ahmad, Sarah Aliah, Chong Choi Yen, Low Sin Yee, Chan Weng Hong, Norhalifah Hanim, Siti Mariam, NurWaliyuddin, Durga, Mallisah, Revathy, Dr. Mohd Fahmi, Noor Aini, Mohamad Faiz, Adrian Wong, Amanda Yeap, and Chew Chui Sze. The helpful and friendly PPSK staffs, Siti Kurunisa, Siti Rosmaizati, Wan Razlin, Wan Mohd Sahnusi, Zulkhairi Bin Othman, Mohd Aminorddin, Roslina Mat Zain, Muhammad Ismail, and Muhammad Syafiq.

Last but not least, I am grateful to every USM staffs, cleaners, security guards, friends, family, and strangers who showed me random acts of kindness at my most difficult times. Thank you.

## TABLE OF CONTENTS

Acknowledgement .....	ii
Table of Contents.....	iii
List of Tables.....	x
List of Figures.....	xi
List of Symbols, Abbreviations and Acronymns .....	xiv
Abstrak.....	xviii
Abstract. ....	xx
CHAPTER ONE: INTRODUCTION.....	1
1.1 Overview .....	1
1.2 Amoebiasis prevalence around the world .....	2
1.3 Biology of <i>E. histolytica</i> .....	5
1.4 Kennedy pathway – CDP-choline pathway .....	9
1.5 Selection of inhibitors targeting choline kinase .....	16
1.6 Gene silencing of <i>E. histolytica</i> .....	24
1.7 Problem statement and rationale of study .....	29
1.8 Aims of study .....	31
CHAPTER TWO: MATERIALS AND METHODS. ....	33
2.1 Materials.....	33
2.1.1 Chemicals .....	33
2.1.2 Molecular biology reagents .....	33
2.1.3 Kits.....	33

2.1.4	Consumables.....	33
2.1.5	General instruments .....	33
2.1.6	<i>Escherichia coli</i> strains and cell line .....	33
2.1.7	Vector.....	34
2.1.8	Computer software.....	34
2.1.9	Oligonucleotides .....	34
2.1.10	Medium, buffers, and solutions preparation.....	47
2.1.10 (a)	<i>E. histolytica</i> TY I -S-33 culture medium.....	47
2.1.10 (b)	Dulbecco's Modified Eagle's medium (DMEM) for use with MTT assay.....	47
2.1.10 (c)	<i>E. histolytica</i> cryoprotectant (2×).....	48
2.1.10 (d)	<i>Escherichia coli</i> Luria Bertani (LB) broth.....	48
2.1.10 (e)	Luria Bertani (LB) agar .....	49
2.1.10 (f)	<i>Escherichia coli</i> competent cells medium .....	49
2.1.10 (g)	Ampicillin .....	50
2.1.10 (h)	Isopropyl β D-1-thiogalactopyranoside (IPTG).....	50
2.1.10 (i)	3-(4,5-Dimethylthiazol-2-yl)-2,5-diphenyltetrazolium bromide (MTT) .....	50
2.1.10 (j)	Amoeba phosphate buffered saline (PBS-A).....	50
2.1.10 (k)	Mowiol mounting medium .....	51
2.1.11	DNA and RNA experiment solutions preparation.....	52
2.1.11 (a)	Tris-acetate-EDTA (TAE) buffer (10×) .....	52
2.1.11 (b)	Ethidium bromide staining solution .....	52
2.1.12	Protein experiment solutions preparation.....	52
2.1.12 (a)	Tris-glycine running buffer (1×) .....	52

2.1.12 (b) Stacking gel buffer (2×).....	53
2.1.12 (c) Resolving gel buffer (4×).....	53
2.1.12 (d) Sodium dodecyl sulfate polyacrylamide gel electrophoresis (SDS-PAGE) sample buffer (2×).....	53
2.1.12 (e) Sodium dodecyl sulfate (SDS) solution (10%).....	53
2.1.12 (f) Ammonium persulfate (APS) (10%).....	54
2.1.12 (g) Coomassie brilliant blue staining solution.....	54
2.1.12 (h) Coomassie brilliant blue destaining solution.....	54
2.1.12 (i) Lysis buffer.....	54
2.1.12 (j) Wash buffer.....	55
2.1.12 (k) Thrombin solution.....	55
2.1.13 Enzymatic assay reagents.....	55
2.1.13 (a) Adenosine triphosphate (ATP).....	55
2.1.13 (b) Bovine serum albumin (BSA).....	56
2.1.13 (c) Potassium chloride (KCl <sub>2</sub> ).....	56
2.1.13 (d) Magnesium chloride (MgCl <sub>2</sub> ).....	56
2.1.13 (e) Manganese chloride (MnCl <sub>2</sub> ).....	57
2.1.13 (f) Nicotinamide adenine dinucleotide (NADH).....	57
2.1.13 (g) Phosphoenolpyruvate (PEP).....	57
2.1.13 (h) Tris-HCl buffer.....	58
2.1.14 Selection of inhibitors.....	58
2.1.15 Preparation of inhibitors.....	58
2.1.15 (a) 2-amino-1-butanol.....	60
2.1.15 (b) Choline kinase $\alpha$ inhibitor, CK37.....	60
2.1.15 (c) Flavopiridol.....	60

2.1.15 (d)H-89 dihydrochloride hydrate.....	60
2.1.15 (e) Hemicholinium-3 (HC-3) .....	60
2.1.15 (f) Hexadecyltrimethylammonium bromide (HDTAB) ...	61
2.1.15 (g) Metronidazole .....	61
2.1.15 (h) Thiamine HCl.....	61
2.2 Methodology .....	61
2.2.1 Molecular biology based methods .....	61
2.2.1 (a) Plasmid isolation from <i>E. coli</i> .....	61
2.2.1 (b) Determination of DNA concentration .....	62
2.2.1 (c) Polymerase chain reaction (PCR) amplification of DNA .....	63
2.2.1 (d) Restriction enzyme digestion .....	64
2.2.1 (e) Heat shock transformation method.....	64
2.2.2 Protein based methods .....	65
2.2.2 (a) Protein expression .....	65
2.2.2 (b) Protein purification.....	65
2.2.2 (c) Determination of protein concentration.....	66
2.2.2 (d) Sodium dodecyl sulfate polyacrylamide gel electrophoresis (SDS-PAGE).....	67
2.2.2 (e) Enzyme kinetics .....	68
2.2.2 (f) Enzyme kinetics data analysis.....	69
2.2.3 Cell culture based methods.....	70
2.2.3 (a) Maintenance of <i>E. histolytica</i> axenic culture.....	70
2.2.3 (b) Cryopreservation and propagation of <i>E. histolytica</i> trophozoites .....	70

2.2.3 (c)	Preparation of <i>E. coli</i> glycerol stock .....	71
2.2.3 (d)	Preparation of <i>E. coli</i> competent cells .....	71
2.2.4	Inhibition of <i>E. histolytica</i> trophozoites with inhibitors .....	72
2.2.4 (a)	Treatment of <i>E. histolytica</i> .....	72
2.2.4 (b)	Cell viability determination by MTT assay .....	72
2.2.5	RNA based methods .....	74
2.2.5 (a)	Preparation of short interfering RNA (siRNA) stock solutions .....	74
2.2.5 (b)	Determination of transfection efficiency .....	74
2.2.5 (c)	siRNA silencing experiment .....	75
2.2.5 (d)	Total RNA extraction from <i>E. histolytica</i> trophozoites .....	75
2.2.5 (e)	Determination of RNA concentration .....	76
2.2.5 (f)	RNA integrity assessment using bleach gel .....	76
2.2.5 (g)	Reverse-transcriptase polymerase chain reaction (RT- PCR) for cDNA synthesis .....	77
2.2.5 (h)	Determination of primer pairs PCR efficiency .....	77
2.2.5 (i)	Gene expression analysis using $\Delta\Delta C_T$ method .....	78
CHAPTER THREE: RESULT .....		79
3.1	Verification of <i>E. histolytica</i> choline kinase and human choline kinase $\alpha 2$ plasmid constructs .....	79
3.1.1	Restriction enzyme analysis .....	79
3.1.2	PCR amplification of EhCK and hCK $\alpha 2$ .....	79



3.2	Expression and purification of <i>E. histolytica</i> choline kinase and human choline kinase $\alpha 2$ .....	82
3.2.1	Expression and purification of EhCK .....	82
3.2.2	Expression and purification of hCK $\alpha 2$ .....	84
3.3	Enzyme kinetics of <i>E. histolytica</i> choline kinase and human choline kinase $\alpha 2$ with magnesium and manganese cofactors.....	84
3.3.1	Determination of EhCK Michaelis-Menten kinetic constants ....	86
3.3.2	Determination of hCK $\alpha 2$ Michaelis-Menten kinetic constants...	89
3.4	Selection of inhibitors.....	89
3.5	Inhibition study of various compounds on EhCK and hCK $\alpha 2$ .....	89
3.5.1	Inhibition of EhCK and hCK $\alpha 2$ by choline kinase $\alpha$ inhibitor (CK37).....	91
3.5.2	Inhibition of EhCK and hCK $\alpha 2$ by flavopiridol.....	91
3.5.3	Inhibition of EhCK and hCK $\alpha 2$ by H-89 dihydrochloride hydrate.....	94
3.5.4	Inhibition of EhCK and hCK $\alpha 2$ by hemicholinium-3 (HC-3) ....	94
3.5.5	Inhibition of EhCK and hCK $\alpha 2$ by hexadecyltrimethylammonium bromide (HDTAB).....	94
3.6	Determination of <i>E. histolytica</i> cell viability after inhibitor treatment ...	98
3.6.1	Growth inhibition of <i>E. histolytica</i> by metronidazole .....	98
3.6.2	Growth inhibition of <i>E. histolytica</i> by flavopiridol .....	100
3.6.3	Growth inhibition of <i>E. histolytica</i> by H-89.....	100
3.6.4	Growth inhibition of <i>E. histolytica</i> by HDTAB .....	100
3.7	siRNA treatment on <i>E. histolytica</i> .....	104
3.7.1	Integrity of purified <i>E. histolytica</i> RNA .....	107

3.7.2	Determination of optimum real-time PCR primers annealing temperature by gradient PCR .....	107
3.7.3	Determination of real-time PCR primer efficiency and specificity .....	107
3.7.4	Determination of optimum siRNA transfection concentration .	111
3.7.5	Determination of gene expression after siRNA treatment .....	111
CHAPTER FOUR: DISCUSSION.....		116
4.1	Roles of cofactor in regulating enzyme conformation .....	117
4.2	Effects of inhibitor on enzyme .....	121
4.3	Effects of inhibitor on <i>E. histolytica</i> trophozoites.....	123
4.4	Gene silencing with siRNA in <i>E. histolytica</i> .....	127
CHAPTER FIVE: CONCLUSION. ....		131
REFERENCES .....		135
APPENDICES		
APPENDIX A - EhCK ORF (XM_652388.1) and amino acid (XP_657480.1) sequences		
APPENDIX B - hCK $\alpha$ 2 ORF (NM_001277.2) and amino acid sequences (NP_001268.2)		
APPENDIX C – pGEX-RB EhCK vector map		
APPENDIX D - Conference proceeding		
APPENDIX E - Research article		

## LIST OF TABLES

	Page
Table 2.1 List of chemicals .....	35
Table 2.2 List of molecular biology reagents.....	38
Table 2.3 List of consumables.....	39
Table 2.4 List of general instruments .....	40
Table 2.5 List of computer softwares .....	43
Table 2.6 List of oligonucleotides .....	44
Table 2.7 Preliminary selection of inhibitors .....	59
Table 3.1 IC <sub>50</sub> values of selected inhibitors for EhCK and hCKα2 with Mg <sup>2+</sup> or Mn <sup>2+</sup> as cofactor. ....	99
Table 3.2 The EC <sub>50</sub> of inhibitors on <i>E. histolytica</i> trophozoites after 48-hour incubation. ....	106

## LIST OF FIGURES

	<b>Page</b>
Figure 1.1 Life cycle of <i>E. histolytica</i> describing invasive and non-invasive infections.....	6
Figure 1.2 Freeze-fracture image of <i>E. histolytica</i> P face and E face.....	8
Figure 1.3 Surface characteristics of <i>E. histolytica</i> . ....	10
Figure 1.4 Composition of phospholipid in whole cells, internal vesicles and plasma membrane of <i>E. histolytica</i> .. ....	11
Figure 1.5 <i>E. histolytica</i> Kennedy pathway illustrating phosphatidylisopropanolamine, phosphatidylethanolamine, and phosphatidylcholine biosynthesis.. ....	12
Figure 1.6 Stereo diagram of hCK $\alpha$ 2 monomer with the binding of ADP (ball-and-stick in cyan) and phosphocholine (ball-and-stick in green).....	14
Figure 1.7 CK inhibitors and their structures.. ....	21
Figure 1.8 Gene silencing mechanism initiated by shRNAs or long dsRNAs .....	26
Figure 1.9 Experimental overview .....	32
Figure 2.1 pGEX-RB vector map and properties.. ....	42
Figure 2.2 The binding site of EhCK siRNA sense and antisense strands on EhCK mRNA.....	45
Figure 2.3 The binding site of EhGAPDH siRNA sense and antisense strands on EhGAPDH mRNA.. ....	46
Figure 3.1 Verification of pGEX RB-EhCK and pGEX RB-hCK $\alpha$ 2 clones by restriction digestion with <i>Nde</i> I and <i>Bam</i> H I .. ....	80

Figure 3.2	Verification of pGEX RB-EhCK and pGEX RB-hCK $\alpha$ 2 clones by PCR.....	81
Figure 3.3	Expression and purification of EhCK protein..	83
Figure 3.4	Expression and purification of hCK $\alpha$ 2 protein.....	85
Figure 3.5	Determination of EhCK Michaelis-Menten constants for choline with magnesium and manganese as the cofactor.....	87
Figure 3.6	Determination of EhCK Michaelis-Menten constants for ATP with magnesium and manganese as the cofactor.....	88
Figure 3.7	Determination of hCK $\alpha$ 2 Michaelis-Menten constants for choline and ATP with magnesium as a cofactor.....	90
Figure 3.8	Inhibition of EhCK and hCK $\alpha$ 2 by CK37.....	92
Figure 3.9	Inhibition of EhCK and hCK $\alpha$ 2 by flavopiridol.....	93
Figure 3.10	Inhibition of EhCK and hCK $\alpha$ 2 by H-89..	95
Figure 3.11	Inhibition of EhCK and hCK $\alpha$ 2 by HC-3.....	96
Figure 3.12	Inhibition of EhCK and hCK $\alpha$ 2 by HDTAB.....	97
Figure 3.13	Determination of EC <sub>50</sub> of 48-hour metronidazole treatment on <i>E. histolytica</i> . ....	101
Figure 3.14	Determination of EC <sub>50</sub> of 48-hour flavopiridol treatment on <i>E. histolytica</i> . ....	102
Figure 3.15	Determination of EC <sub>50</sub> of 48-hour H-89 treatment on <i>E. histolytica</i> . ....	103
Figure 3.16	Determination of EC <sub>50</sub> of 48-hour HDTAB treatment on <i>E. histolytica</i> . ....	105
Figure 3.17	Integrity of purified <i>E. histolytica</i> RNA.....	108

Figure 3.18	Determination of optimum annealing temperature for real-time PCR primers by gradient PCR.. .....	109
Figure 3.19	Determination of real-time PCR primers efficiency. ....	110
Figure 3.20	Determination of real-time PCR primers specificity.. .....	112
Figure 3.21	Determination of optimum siRNA concentration using siGLO RISC-Free Control siRNA. ....	113
Figure 3.22	Relative gene expression after silencing experiment. ....	114

## LIST OF SYMBOLS, ABBREVIATIONS AND ACRONYMS

×	Multiply/Times
°C	Degree Celsius
μL	Microlitre
μm	Micrometre
μM	Micromolar
ADP	Adenosine diphosphate
ALA	Amoebic liver abscess
APS	Ammonium persulfate
ATP	Adenosine triphosphate
BLAST	Basic Local Alignment Search Tool
Bp	Base pair
BSA	Bovine serum albumin
CAEP	Ceramide aminoethyl phosphonate
CCT	Choline phosphate cytidyltransferase
cDNA	Complementary deoxyribonucleic acid
CDP-Choline	Cytidine diphosphocholine
CDP-Etn	Cytidine diphosphoethanolamine
CDP-Ispn	Cytidine diphosphoisopropanolamine
CK	Choline kinase
DAG	1,2- <i>sn</i> -diacylglycerol
DMSO	Dimethyl sulfoxide
DNA	Deoxyribonucleic acid
dNTP	Deoxyribonucleotide triphosphate

DsiRNA	Dicer substrate ribonucleic acid
dsRNA	Double stranded ribonucleic acid
EDTA	Ethylenediaminetetraacetic acid
EhCK	<i>Entamoeba histolytica</i> choline kinase
ELISA	Enzyme-linked immunosorbent assay
Etn	Ethanolamine
Etn-P	Phosphoethanolamine
<i>G</i>	Gravity force
Gal/GalNac	Galactose/N-acetylgalactosamine
GAPDH	Glyceraldehyde 3-phosphate dehydrogenase
gDNA	Genomic deoxyribonucleic acid
GST	Glutathione S-transferase
H	Hour
HC-3	Hemicholinium-3
hCK	Human choline kinase
HCl	Hydrochloric acid
HDTAB	Hexadecyltrimethylammonium bromide
IHA	Indirect haemagglutination assay
IPTG	Isopropyl $\beta$ -D-1-thiogalactopyranoside
Ispn	Isopropanolamine
Ispn-P	Phosphoisopropanolamine
kDa	Kilo Dalton
$K_m$	Michaelis-Menten constant
L	Liter
LB	Luria-Bertani



LDH	Lactate dehydrogenase
Min	Minutes
miRNA	Micro ribonucleic acid
mL	Millilitre
mRNA	Messenger ribonucleic acid
NADH	Nicotinamide adenine dinucleotide (reduced form)
NCBI	National Center for Biotechnology Information
Nm	Nanometer
Nt	Nucleotides
OD	Optical density
PA	Phosphatidic acid
PBS-A	Amoeba phosphate buffered saline
PC	Phosphocholine
PCR	Polymerase chain reaction
PEMT	Phosphatidylethanolamine <i>N</i> -methyltransferase
PEP	Phosphoenolpyruvate
PfCK	<i>Plasmodium falciparum</i> choline kinase
PI	Phosphatidylinositol
PK	Pyruvate kinase
PS	Phosphatidylserine
PtdCho	Phosphatidylcholine
PtdEtn	Phosphatidylethanolamine
PtdIspn	Phosphatidlisopropanolamine
qPCR	Quantitative PCR
RISC	RNA-induced silencing complex

RNAi	Ribonucleic acid interference
Rpm	Revolutions per min
RT-PCR	Reverse transcription-polymerase chain reaction
S	Second
SDS-PAGE	Sodium dodecyl sulfate-polyacrylamide gel electrophoresis
shRNA	Short hairpin ribonucleic acid
siRNA	Short interfering ribonucleic acid
SOD	Superoxide dismutase
TAE	Tris-acetate-ethylenediaminetetraacetic acid
<i>Taq</i>	<i>Thermus aquaticus</i>
TEMED	Tetramethylethylenediamine
T <sub>m</sub>	Melting temperature
U	Unit
UV	Ultraviolet
v/v	Volume to volume
V <sub>max</sub>	Maximum velocity
w/v	Weight to volume
WHO	World Health Organization

# PERENCATAN KOLINA KINASE SEBAGAI SUATU PENDEKATAN ANTIAMOEBIK DALAM *ENTAMOEBIA HISTOLYTICA*

## ABSTRAK

*Entamoeba histolytica* (*E. histolytica*) ialah parasit punca amoebiasis yang menyebabkan penyakit kolitis ameba atau abses hati ameba. Pesakit dijangkiti amoebiasis dalam usus diberi rawatan dengan ubat metronidazole. Adalah dikhuatiri bahawa kekerapan penggunaan metronidazole dalam rawatan amoebiasis akan mewujudkan rintangan metronidazole dalam *E. histolytica*. Pendekatan baharu dalam rawatan menggunakan laluan CDP-kolina diterokai dalam kajian ini. Kajian perencatan dilakukan melalui kaedah perencatan enzim EhCK oleh perencat CK dan “knockdown” mRNA EhCK dengan kaedah “RNA interference”. Kolina kinase *E. histolytica* (EhCK) mengutamakan penggunaan kofaktor  $Mn^{2+}$  berbanding dengan  $Mg^{2+}$  yang selalunya diutamakan dalam CK spesis lain termasuklah manusia. Perbezaan dalam pengutamaan kofaktor  $Mn^{2+}$  berkemungkinan wujudnya perencat EhCK yang tidak menjejaskan enzim CK manusia (hCK). Nilai  $K_m$  dan  $V_{max}$  enzim EhCK dan hCK $\alpha$ 2 melibatkan kofaktor  $Mn^{2+}$  atau  $Mg^{2+}$  ditentukan melalui cara spektrofotometri asai gabungan piruvat kinase-laktat dehidrogenase (PK-LDH). Nilai  $IC_{50}$  EhCK dan hCK $\alpha$ 2 ditentukan selepas kajian melibatkan beberapa perencat CK komersial (CK37, HC-3, HDTAB, flavopiridol, dan H-89). Hanya beberapa perencat dipilih untuk diuji ke atas trofozoit *E. histolytica* selama 48 jam bagi menentukan nilai  $EC_{50}$  setiap perencat. Kaedah perendaman siRNA dupleks digunakan untuk melenyapkan ekspresi gen EhCK. Jumlah ekspresi gen ditentukan melalui “real-time qPCR”. Kecekapan transfeksi siRNA ditentukan dengan pendarfluor siGLO RISC-Free Control siRNA. Nilai  $K_m$  dan  $V_{max}$  EhCK dengan kofaktor  $Mn^{2+}$  bagi kolina ialah  $0.12 \pm 0.030$  mM

and  $34.12 \pm 1.87$  U/mg; bagi ATP pula, nilai  $K_m$  dan  $V_{max}$  ialah  $1.61 \pm 0.26$  mM dan  $48.98 \pm 2.14$  U/mg. Aktiviti EhCK kurang cekap dengan kofaktor  $Mg^{2+}$ . Nilai  $K_m$  didapati lebih tinggi ( $0.20 \pm 0.044$  mM bagi kolina;  $10.85 \pm 2.33$  mM bagi ATP) manakala nilai  $V_{max}$  didapati menyusut ( $2.13 \pm 0.14$  U/mg bagi kolina;  $3.02 \pm 0.37$  U/mg bagi ATP). Nilai  $K_m$  dan  $V_{max}$  hCK $\alpha$ 2 dengan kofaktor  $Mg^{2+}$  bagi kolina ialah  $0.12 \pm 0.012$  mM dan  $71.4 \pm 1.54$  U/mg; manakala ATP pula ialah  $0.67 \pm 0.085$  mM and  $113.6 \pm 5.13$  U/mg. Berdasarkan nilai  $IC_{50}$  bagi kedua-dua enzim EhCK dan hCK $\alpha$ 2, hanya tiga perencat enzim, CK37 ( $60.64 \pm 14.67$   $\mu$ M vs  $IC_{50}$  untuk hCK $\alpha$ 2  $68.41 \pm 12.08$   $\mu$ M), flavopiridol ( $45.51 \pm 15.50$   $\mu$ M vs  $IC_{50}$  untuk hCK $\alpha$ 2  $297.0 \pm 80.50$   $\mu$ M), dan H-89 ( $100.60 \pm 17.41$   $\mu$ M vs  $IC_{50}$  untuk hCK $\alpha$ 2  $392.1 \pm 36.62$   $\mu$ M) lebih efektif terhadap EhCK berbanding dengan hCK $\alpha$ 2. Semua perencat yang diuji kurang berkesan dengan kofaktor  $Mn^{2+}$  berbanding dengan kofaktor  $Mg^{2+}$ . Kajian ke atas trofozoit menunjukkan hanya perencat HDTAB, H-89 dan metronidazole yang masing-masing mempunyai nilai  $EC_{50}$   $47.40 \pm 7.22$   $\mu$ M,  $32.44 \pm 5.05$   $\mu$ M, dan  $1.73 \pm 0.33$   $\mu$ M, berjaya mengakibatkan kematian trofozoit selepas 48 jam. Kecekapan transfeksi paling tinggi ialah 55% selepas merendam siGLO RISC-Free Control siRNA sebanyak 10  $\mu$ g/mL selama 16 jam. Kepekatan 10  $\mu$ g/mL digunakan dalam eksperimen transfeksi melibatkan siRNA kawalan positif GAPDH, siRNA EhCK, dan siRNA bukan sasaran GFP. Hasilnya ekspresi gen GAPDH menyusut sebanyak 99%, manakala ekspresi gen EhCK menyusut sebanyak 47% selepas transfeksi. Kajian ini telah mengenal pasti prencat EhCK dan siRNA yang berpotensi untuk diubahsuaikan bagi meningkatkan keberkesanan terhadap EhCK tanpa menjejaskan hCK. Penggunaan perencat dan siRNA yang khusus terhadap EhCK merupakan suatu pendekatan yang baru dalam menghalang tumbesaran *E. histolytica* melalui gangguan pada laluan biosintesis fosfolipid parasit tersebut.

# INHIBITION OF CHOLINE KINASE AS AN ANTIAMOEBIIC APPROACH IN *ENTAMOEBA HISTOLYTICA*

## ABSTRACT

*Entamoeba histolytica* is the causative parasite for amoebiasis which manifests into amoebic colitis or amoebic liver abscess. Patients with intestinal amoebiasis are traditionally treated with metronidazole. There is concern for metronidazole resistance and the resistance pathway has been discovered in *E. histolytica*. A new antiamoebic approach via CDP-choline pathway is explored in this study. Inhibition studies were carried out by inhibition of EhCK enzyme by some potential CK inhibitors and via EhCK gene knockdown using RNA interference. *E. histolytica* choline kinase (EhCK) showed preference for  $Mn^{2+}$  as cofactor instead of  $Mg^{2+}$  that is usually used by choline kinases from other species including human. The unique preference for  $Mn^{2+}$  suggests the possibility of EhCK specific inhibitors not affecting the human host CK (hCK).  $K_m$  and  $V_{max}$  of purified EhCK and hCK $\alpha 2$  proteins were determined by pyruvate kinase-lactate dehydrogenase (PK-LDH) coupled assay with  $Mn^{2+}$  or  $Mg^{2+}$  as cofactors. The  $IC_{50}$  values for EhCK and hCK $\alpha 2$  were determined with several commercial CK inhibitors (CK37, HC-3, HDTAB, flavopiridol, and H-89). Selected inhibitors were incubated with *E. histolytica* trophozoites for 48 hours to determine the  $EC_{50}$  for each inhibitor. Silencing of gene encoding EhCK was carried out using duplex siRNA via soaking method and the gene expression level was measured by real-time qPCR. Transfection efficiency was assessed with fluorescence siGLO RISC-Free Control siRNA. Values of  $K_m$  and  $V_{max}$  of EhCK with  $Mn^{2+}$  as cofactor for choline substrate were  $0.12 \pm 0.030$  mM and  $34.12 \pm 1.87$  U/mg, respectively. For ATP substrate, the  $K_m$  and  $V_{max}$  were  $1.61 \pm 0.26$  mM and  $48.98 \pm 2.14$  U/mg, respectively. EhCK was

much less efficient with  $Mg^{2+}$  cofactor. The  $K_m$  values were higher ( $0.20 \pm 0.044$  mM for choline;  $10.85 \pm 2.33$  mM for ATP) and the  $V_{max}$  decreased ( $2.13 \pm 0.14$  U/mg for choline;  $3.02 \pm 0.37$  U/mg for ATP).  $K_m$  and  $V_{max}$  hCK $\alpha$ 2 in  $Mg^{2+}$  for choline substrate were  $0.12 \pm 0.012$  mM and  $71.4 \pm 1.54$  U/mg, respectively and for ATP substrate the values for  $K_m$  and  $V_{max}$  were  $0.67 \pm 0.085$  mM and  $113.6 \pm 5.13$  U/mg, respectively. Based on  $IC_{50}$  values for EhCK and hCK $\alpha$ 2, three inhibitors, namely CK37 ( $60.64 \pm 14.67$   $\mu$ M vs  $IC_{50}$  for hCK $\alpha$ 2  $68.41 \pm 12.08$   $\mu$ M), flavopiridol ( $45.51 \pm 15.50$   $\mu$ M vs  $IC_{50}$  for hCK $\alpha$ 2  $297.0 \pm 80.50$   $\mu$ M), and H-89 ( $100.60 \pm 17.41$   $\mu$ M vs  $IC_{50}$  for hCK $\alpha$ 2  $392.1 \pm 36.62$   $\mu$ M) were more potent against EhCK than hCK $\alpha$ 2. All inhibitors tested also exhibited lower potency with  $Mn^{2+}$  as the cofactor compared to  $Mg^{2+}$ . Trophozoites growth inhibition showed that only HDTAB, H-89 and control drug metronidazole with  $EC_{50}$  values of  $47.40 \pm 7.22$   $\mu$ M,  $32.44 \pm 5.05$   $\mu$ M, and  $1.73 \pm 0.33$   $\mu$ M, respectively, could penetrate and induce cell death after 48-hour incubation. The highest transfection efficiency of 55% was obtained after soaking with 10  $\mu$ g/mL of siGLO RISC-Free Control siRNA for 16 hours. siRNA concentration of 10  $\mu$ g/mL was used for the transfection of positive control GAPDH, EhCK, and non-targeting GFP siRNAs. RNAi experiment concluded with positive control GAPDH downregulated by 99% while the level EhCK mRNA was downregulated by 47%. This study has identified potential EhCK inhibitors and siRNA for further modifications and testing to achieve higher potency against EhCK but not affecting hCK. The use of specific inhibitors and siRNA targeting EhCK could be novel approach to inhibit the growth of *E. histolytica* by interrupting the phospholipid synthesis pathway of this parasite.

## CHAPTER ONE

### INTRODUCTION

#### 1.1 Overview

Amoebiasis is an infectious disease caused by the parasitic *Entamoeba histolytica*. Centers for Disease Control and Prevention (CDC) reports that only 10% - 20% of *E. histolytica* infections are symptomatic, with asymptomatic cases possibly caused by the non-invasive *E. dispar*. Symptoms range from mild, such as loose faeces, stomach pain; to severe, such as amoebic dysentery (stomach pain, bloody stools, and fever) and amoebic liver abscess. Most infections happen via contaminated water and food sources due to inadequate sanitary facilities. It has been estimated that amoebiasis causes about 50,000 deaths globally (Jensen, 2015). The best way to eradicate this disease is to have good hygiene practices such as frequent hand washing and access to uncontaminated drinking water, apart from providing a clean and safe water source to the community. However, with at least 2 billion people globally drinking water from sources contaminated with faeces, amoebiasis and other water-borne diseases continue to be a threat to the bottom billions (WHO and UNICEF, 2017).

Amoebiasis is routinely treated with nitroimidazole drugs, such as metronidazole and tinidazole. Cysts and trophozoites found in the intestine are treated with a combination of metronidazole and luminal agent. Due to the low cost and effectiveness of nitroimidazole drugs against anaerobic parasites, metronidazole has been the drug of choice for the past half a century. This raises a concern among physicians and scientists that metronidazole-resistance might develop if it is being used as a prophylaxis against

the non-invasive *E. dispar*, a morphologically similar species to *E. histolytica* that co-exist in the human body (Löfmark et al., 2010).

This study focuses on targeting one of the phospholipid synthesis pathway of *E. histolytica* – the CDP-choline pathway as a new anti-amoebic approach. Inhibition was performed at two levels. *In vitro* inhibition at the protein level uses selected compounds that target recombinant *E. histolytica* choline kinase (EhCK), whereas *in vivo* inhibition at the mRNA level uses synthetic short interfering RNA (siRNA) which specifically targets EhCK mRNA. Apart from investigating the prospect of CDP-choline pathway as a new target for amoebiasis treatment, this study would also give an insight on the biochemistry and enzymatic properties of EhCK.

## **1.2 Amoebiasis prevalence around the world**

Amoebiasis has higher prevalence in areas with poor sanitation facilities and its effects are more severe in children living in endemic areas (Anuar et al., 2012, Ximénez et al., 2009). The true prevalence of *E. histolytica* has been overestimated due to morphological bias with the non-pathogenic *E. dispar* and *E. moshkovskii* (Haque et al., 2003). The prevalence data collected previously from asymptomatic individuals were mostly based on microscopic examination of cyst or trophozoites in stool that does not give a clear distinction between these species (Tshalaia, 1941, Clark and Diamond, 1991, Diamond and Clark, 1993). To clearly identify these species, molecular methods such as PCR, antigen-antibody detection with ELISA, and isoenzyme analysis are used in diagnosis (Stanley, 2003).



A study in Mexico which utilizes indirect hemagglutination assay (IHA) found that out of 60,000 serum samples, about 5,600 were positive, which translated to 8.4% *E. histolytica* prevalence in Mexico (Caballero-Salcedo et al., 1994). The seroprevalence of *E. histolytica* infection varied by region in such that children living in an area with better water supply in South Africa was found to be infected by 2% of both *E. dispar* and *E. histolytica* but 50% of children living in areas with inferior sanitation was found to be infected by *E. dispar* alone (Jackson et al., 2000). The overall prevalence of *E. histolytica* infection in South Africa based on a 5-year study period using stool culture and isoenzyme analysis was 2.4%, with more amoebic liver abscess (ALA) cases reported (Stauffer et al., 2006). Faecal antigen ELISA detection employed in the rural area of Egypt found that prevalence of *E. histolytica* (21.4%) is slightly lower than *E. dispar* (24.2%) (Abd-Alla et al., 2000). Meanwhile in Cairo, amoebic colitis was present in 38% of acute diarrhoea patients with positive *E. histolytica* serology test (Abd-Alla and Ravdin, 2002).

In Malaysia, the prevalence study of amoebiasis was carried out among the aborigine communities using polymerase chain reaction (PCR) (Anuar et al., 2012). It was found that 3.2% of the *Entamoeba*-infected population investigated was due to *E. histolytica* whereas *E. dispar* and *E. moshkovskii* species were at 13.4% and 1.0%, respectively. A study in a Philippines mental institution, also using PCR detection method, had higher *E. histolytica* prevalence at 65.5% compared to 5.3% of *E. dispar* infected patients (Rivera et al., 2006). ALA incidence reported in Hue, Vietnam between 1990-1998 was at an average of 21 cases in 100,000 individuals per year. Commercially available ELISA detection carried out among the ALA patients in an area in Hue City had unexpectedly low prevalence of 0.9% for *E. histolytica* (Blessmann et al., 2002).

While this finding is common in other endemic areas, it suggests that local factors such as gut flora or diet contribute to the infection. Similarly using ELISA, investigation in an urban slum area of Dhaka, Bangladesh showed that 80% of children participated in the study were infected by *E. histolytica* resulting to an incidence rate of 0.45 infection per child per year. However only a-fifth of the children had *E. histolytica* associated diarrhoea or dysentery. That study also showed that a repeat infection was seen in 53% of the children (Haque et al., 2006).

Although infection is commonly associated with poor hygiene practices, contaminated water, and inadequate sanitization, there are other ways where *E. histolytica* is transmitted. A study in Australia conducted using PCR detection method showed that there were 3.4% of *E. histolytica* prevalence rate, 33.7% and 24.7% of *E. dispar* and *E. moshkovskii* respectively, although presence of the 3 *Entamoeba* species concurrently was more prevalent. Patients in Australia were associated with risk factors of travelling to endemic areas and homosexual men (Fotedar et al., 2007). Travelers to endemic areas are exposed via consumption of not properly cooked food, predominantly cold beverage, ice-cream and raw fruit on ice (De Lalla et al., 1992). In countries such as Japan, Taiwan, China, and South Korea, studies have shown that there has been an increased prevalence of *E. histolytica* among human immunodeficiency virus (HIV) patients other than intestinal parasites *Cryptosporidium sp*, *Microsporidia sp*, *Isospora belli*, and *Cyclospora cayetenesis* (Teklemariam et al., 2013). There is increasing prevalence of invasive amoebiasis among HIV patients and emerging concern that *E. histolytica* is spreading as sexually transmitted infections, among men who have sex with men, and female commercial sex workers (Yanagawa et al., 2016, Abdollahi et al., 2015, Hung et al., 2008, Ohnishi

et al., 2004). Physicians are advised to be aware of the complications and possibilities of invasive amoebiasis present in HIV patients. Measures should also be taken to prevent widespread of infection in non-endemic area.

### **1.3 Biology of *E. histolytica***

*E. histolytica*, one of the parasitic amoebas is a protozoon. Its life cycle is relatively simple and consists of two stages: the trophozoite stage and the cyst stage (Figure 1.1). The most common route of transmission is the faecal-oral route via cysts. Once cysts are ingested via *E. histolytica* contaminated water or food, the quadrinucleate cyst survives acidic stomach condition and travels to the alkaline terminal ileum to release eight feeding trophozoites in the large intestine. From here, there is a 90% probability that the infection is non-invasive. In non-invasive infection, after encystation occurs, trophozoites colonize the large intestine and reproduce by binary fission. Binary fission continues until encystation is triggered by gal/GalNAc lectin, mucin glycoproteins or other bacteria (Petri Jr et al., 2002). The cysts, and some trophozoites are then passed out from the body via faeces. Patients that have non-invasive infection might present symptoms such as diarrhoea and stomach discomfort.

Patients that present symptoms such as bloody/watery diarrhoea, abdominal pain and tenderness, might be at risk of invasive amoebiasis. Only 10% of infection might develop into invasive amoebiasis. This happens when the colonized trophozoites start penetrating intestinal mucin layer and trophozoite lectin attaches directly to *N*-acetyl-D-galactosamine, triggering a cascade of events that leads to host cell death. Once the

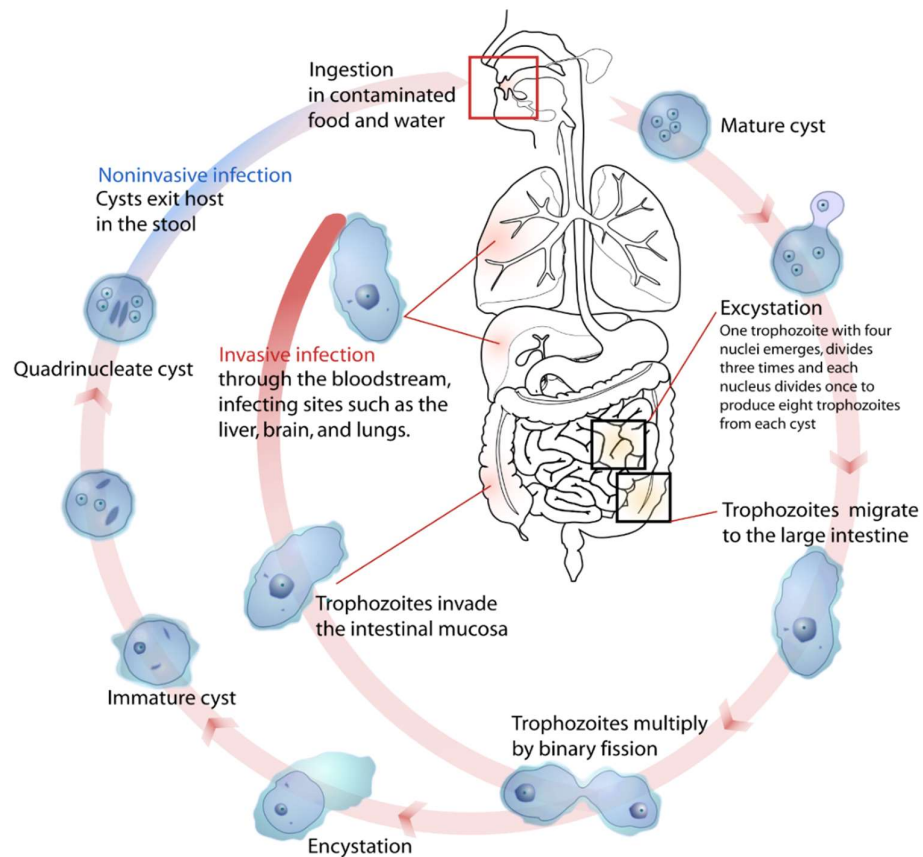


Figure 1.1 Life cycle of *E. histolytica* describing invasive and non-invasive infections (Villarreal, 2008).

intestinal epithelial surface ruptures, trophozoites move into the blood stream that allows them to travel to other organs such as liver, lungs, and (less likely) brain, causing abscesses (Hasudungan, 2013). Amoebic liver abscess (ALA) is the most common form of extraintestinal amoebiasis. Invasive amoebiasis is treated with nitroimidazoles, particularly metronidazole whereas non-invasive infection is treated with paromomycin (Haque et al., 2003).

*E. dispar* which has morphological similarities with *E. histolytica* under microscopic examination might account for 90% of the non-invasive infections. By using antigenic and serological tests, it has been found that infection of the non-pathogenic *E. dispar* is 10 times more common than *E. histolytica*. Experts recommend that microscopically determined amoebiasis should not be treated unless *E. histolytica* is present in the patient. This is to reduce unnecessary drug use on *E. dispar* infections that does not cause any diseases and prevent drug resistance (Clark, 2000).

*E. histolytica* trophozoites are extremely sensitive to physiochemical environment changes. Rounded trophozoites measure between 7  $\mu$ M – 40  $\mu$ M, with larger trophozoites (20  $\mu$ M – 40  $\mu$ M) found in amoebas obtained from liver or intestine and smaller ones (7  $\mu$ M – 30  $\mu$ M) found in non-dysenteric stools or in culture (Martínez-Palomo, 1982). The plasma membrane of *E. histolytica* is about 10 nm thick (thicker than most mammalian cells) with the protoplasmic face (P face) of the plasma membrane in contact with ectoplasm consists of abundant and heterogeneous population of membrane particles such as integral proteins. The complementary extracellular face (E face) has lesser population of membrane particles (Figure 1.2). Under SEM examination, the surface of trophozoites has wrinkled morphology with

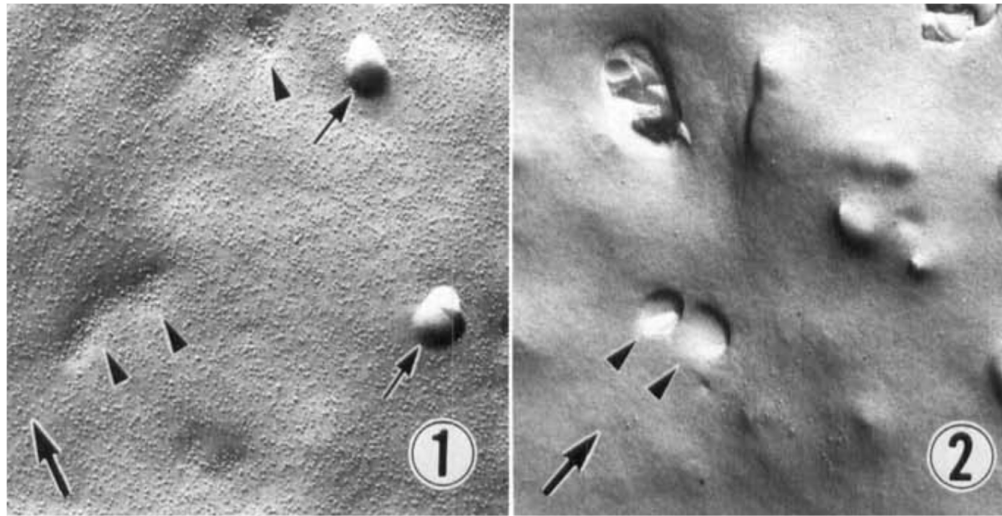


Figure 1.2 Freeze-fracture image of *E. histolytica* P face (1) and E face (2). Like most of the eukaryotic cells, intramembranous particles are found more abundant on the P face (1) than the E face (2). Particle-rich depressions on P and E faces are indicated by arrowheads whereas particle-free small protrusions are indicated by arrows. Arrows on the bottom left corner indicates direction of shadowing (Yoshikawa et al., 1988).

circular openings, a diameter of 0.2  $\mu\text{M}$  – 0.4  $\mu\text{M}$  which corresponds to the mouths of micropinocytic vesicles (Figure 1.3) (Martínez-Palomo, 1982).

The membrane of *E. histolytica* trophozoite consists of several phospholipids (Figure 1.4). The major phospholipid identified is phosphatidylcholine (PtdCho), followed by other species such as phosphatidic acid (PA), phosphatidylinositol (PI), phosphatidylserine (PS), ceramide aminoethyl phosphonate (CAEP), phosphatidylethanolamine (PtdEtn), sphingomyelin and other unidentified minor species (Aley et al., 1980). PtdCho is the major phospholipid species in whole cells and internal vesicles, followed by the second abundant CAEP and PtdEtn that are majorly located at the plasma membrane (Aley et al., 1980).

#### **1.4 Kennedy pathway – CDP-choline pathway**

The eukaryotic cell membrane is a phospholipid bilayer that is made up of different phospholipid species. Kennedy pathway consists of CDP-ethanolamine and CDP-choline pathways. The CDP-choline and CDP-ethanolamine pathway is responsible for production of phosphatidylcholine (PtdCho) and phosphatidylethanolamine (PtdEtn), respectively (Figure 1.5).

Both PtdCho and PtdEtn species are found ubiquitously in eukaryotes and several prokaryotes (Fagone and Jackowski, 2013). There are several ways of choline phospholipid metabolism. PtdCho formation via CDP-choline pathway starts from phosphorylation of cytosolic choline by choline kinase (CK). Phosphocholine (PC) is then converted to CDP-choline by choline phosphate cytidyltransferase (CCT). Finally, cytidine monophosphate is replaced with 1,2-*sn*-diacylglycerol (DAG) by

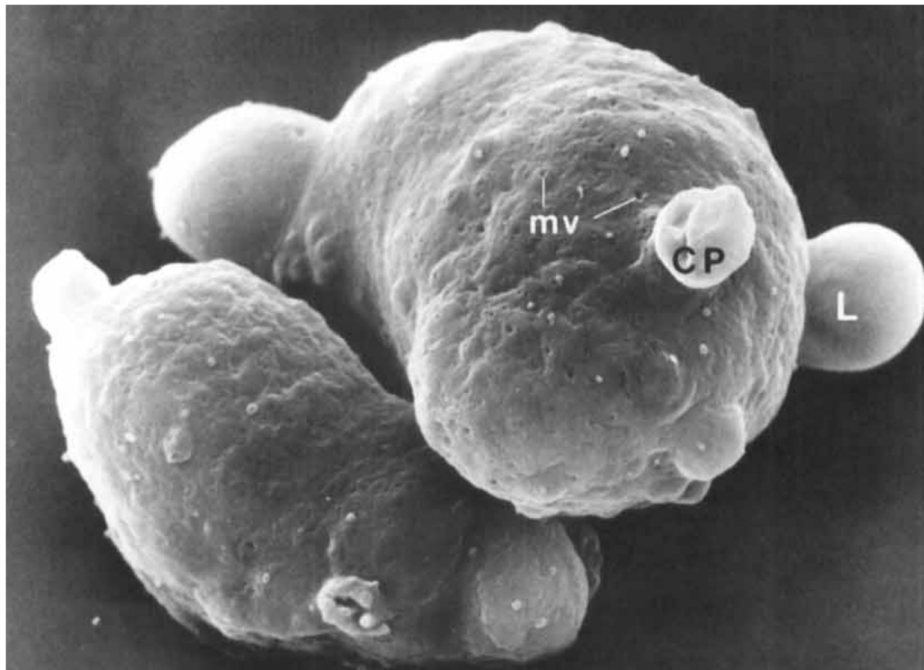


Figure 1.3 Surface characteristics of *E. histolytica*. Seen in this image are minute openings that are known as micropinocytic vesicles (mv), lobopodia (L), and cytoplasmic protrusions (CP) (Gonzales-Robles and Martinez-Palomo, 1983).



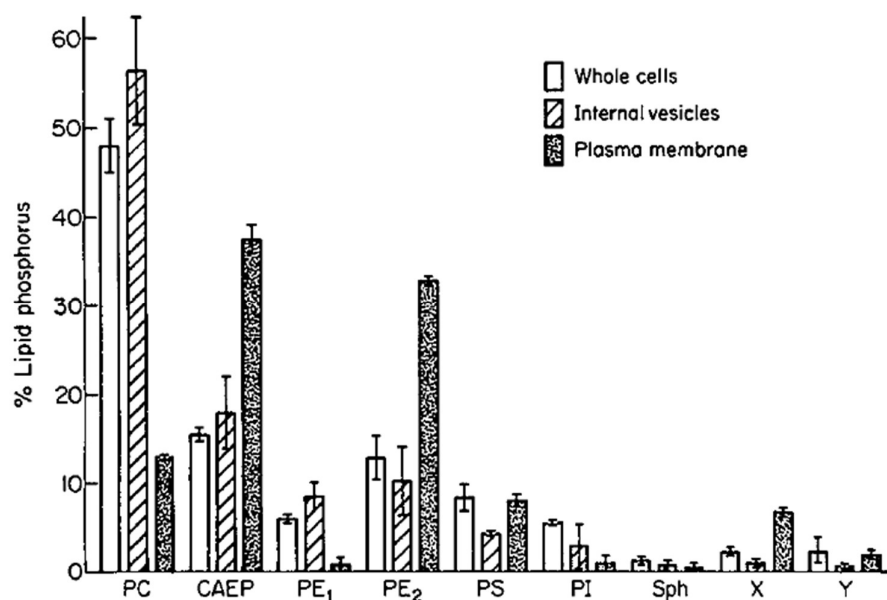


Figure 1.4 Graph represents composition of phospholipid in whole cells, internal vesicles and plasma membrane of *E. histolytica*. PC: PtdCho; CAEP: ceramide aminoethyl phosphonate; PE: PtdEtn; PS: phosphatidylserine; PI: phosphatidylinositol; Sph: sphingomyelin; X,Y: 2 unidentified phospholipids (Aley et al., 1980).

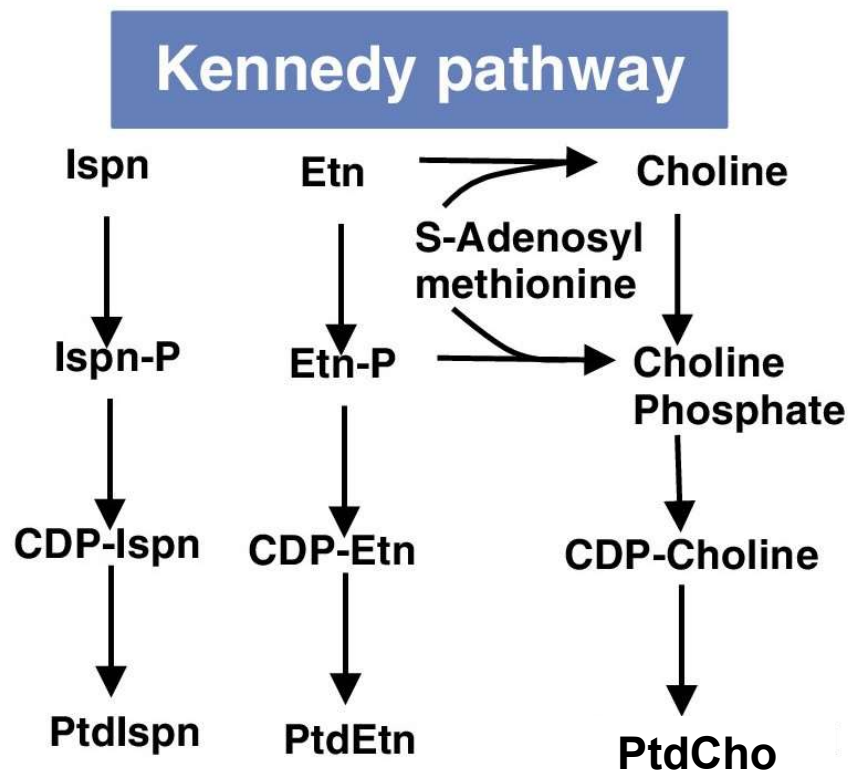


Figure 1.5 *E. histolytica* Kennedy pathway illustrating phosphatidylisopropanolamine, phosphatidylethanolamine, and phosphatidylcholine biosynthesis. Ispn: isopropanolamine; Ispn-P: phosphoisopropanolamine; CDP-Ispn: cytidine diphosphoisopropanolamine; PtdIspn: phosphatidylisopropanolamine; Etn: ethanolamine; Etn-P: phosphoethanolamine; CDP-Etn: cytidine diphosphoethanolamine; PtdEtn: phosphatidylethanolamine; CDP-choline: cytidine diphosphocholine; PtdCho: phosphatidylcholine (Jeelani and Nozaki, 2014).

diacylglycerol cholinephosphotransferase (CPT) and PtdCho is formed. Another method involves *de novo* synthesis of choline, which is through the methylation of PE by phosphatidylethanolamine *N*-methyltransferase (PEMT), using 3 equivalents of *S*-adenosylmethionine (SAM) (Smith, 1993). In mammals, the methylations occur mainly in the liver that produces 30% of hepatic PtdCho. Abolishment of PEMT activity does not cause any physiological changes in mice when coupled with dietary choline deficiency, however, it causes failure to synthesize PtdCho. This in turns decreases the PtdCho:PtdEtn ratio and increases the membrane permeability which leads to liver failure (Vance et al., 2007).

CK and ethanolamine kinase (EK) are the first enzymes in the CDP-choline/ethanolamine pathway to produce PtdCho and PtdEtn. In mammals, CK exists in 3 different isoforms which are produced by 2 different genes. *CHKA* encodes CK $\alpha$  which has 2 different splice variants whereas *CHKB* encodes CK $\beta$  which is 60% homologous to CK $\alpha$  (Aoyama et al., 1998). These isoforms may present as homo/hetero dimers or tetramers in solution (Aoyama et al., 2004). The upregulation of CK $\alpha$  has been closely associated with tumorigenesis (Gallego-Ortega et al., 2009) whereas CK $\beta$  deficiency leads to muscle dystrophy and neonatal bone deformity in mice (Sher et al., 2006).

The structure of CK from *C. elegans* was first elucidated by Peisach and team (2003). The structures of *C. elegans* CK (CKA-2) and hCK $\alpha$ 2 have a typical eukaryotic protein kinase fold (Peisach et al., 2003). They differ at residues 262-281 (of hCK $\alpha$ 2), a region with no catalytic relevance. Here, hCK $\alpha$ 2 has an  $\alpha$ -helix while CKA-2 has 2 short  $\beta$ -strands instead (Figure 1.6). The C-terminal domain contains many conserved and

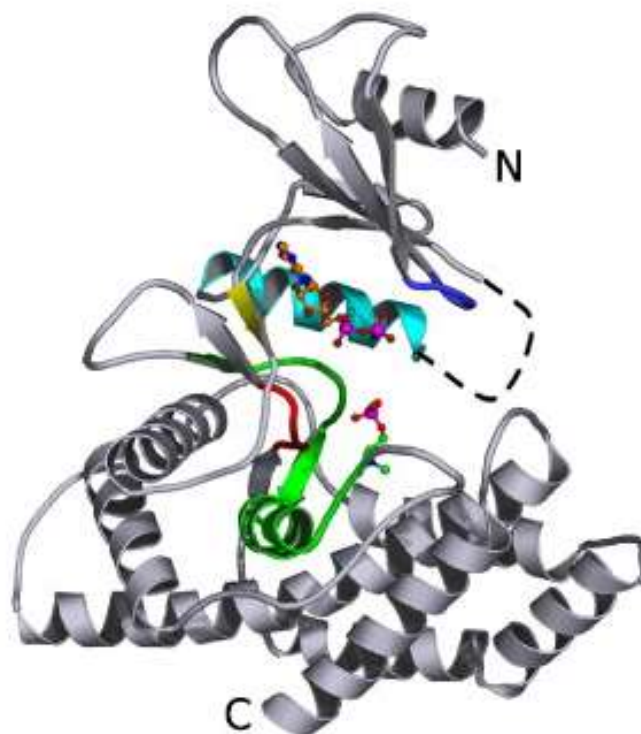


Figure 1.6 Stereo diagram of hCK $\alpha$ 2 monomer with the binding of ADP (ball-and-stick in cyan) and phosphocholine (ball-and-stick in green). Blue: ATP binding loop; Cyan: dimer interface  $\alpha$ -helix; Yellow: short  $\beta$ -strand links N and C-terminal domains; Red: Brenner's motif; Green: choline kinase motif (Malito et al., 2006).

functional regions such as Brenner's motif (302-311), choline kinase motif (326-349), ATP-binding loop (107-114), dimer interface (175-190), and  $\beta$ -strand link (201-204) (Malito et al., 2006).

Due to the involvement of CK and the role of its metabolite, PtdCho in phospholipid of most eukaryotic cells, it became an interesting anti-protozoan target in parasites such as *Plasmodium falciparum*, *Entodinium caudatum*, *Leishmania infantum*, and *Theileria equi* (Gopalakrishnan et al., 2016, Pulido et al., 2017, Bygrave and Dawson, 1976). Notably in *P. falciparum*, the infection increases erythrocyte phospholipid content by 500%, mostly attributed to *Plasmodium* phospholipids (Sherman, 1979). Forty five percent of the increased phospholipids consisted of PtdCho (Vial and Ancelin, 1998). Since the discovery and identification of CK and EK in 1986, efforts to characterize and inhibit PfCK as an antimalarial target is currently underway (Ancelin and Vial, 1986, Choubey et al., 2006, Zimmerman et al., 2013, Serrán-Aguilera et al., 2016).

Using similar approach, this study focuses on *E. histolytica* CK (EhCK) as a target to inhibit trophozoite proliferation. The sequencing of *E. histolytica* genome revealed metabolic pathways present in the species. The presence of these pathways allow development of new chemotherapeutic drugs and targets for anti-amoebic agents (Loftus et al., 2005). EhCK and EhEK have been characterized in the previous study by Chang (2012). Unlike other CKs that may phosphorylate substrate ethanolamine (Gibellini and Smith, 2010), EhCK was proven to be choline specific and was active between 37°C - 42°C. It has a narrow pH activity between pH 7.0- pH 8.5, with optimum activity at pH 8.0 (Chang, 2012). The preference of alkaline condition of EhCK is consistent with other CKs (Gee and Kent, 2003). Metabolomic analysis based

on the reassembly and reannotation of *E. histolytica* genome in 2010 reveals that the Kennedy pathway of *E. histolytica* includes CDP-choline, CDP-ethanolamine, and CDP-isopropanolamine pathways (Figure 1.5). *E. histolytica* trophozoite has PtdCho as its major phospholipid species with CAEP and PtdEtn most abundant in the cell membrane (Aley et al., 1980).

### **1.5 Selection of inhibitors targeting choline kinase**

Choline kinase is an important target in rheumatoid arthritis, malaria, and cancer. CK inhibitors prevent cartilage destruction in rheumatoid arthritis by suppressing aggressive behavior of fibroblast-like synoviocytes from migration and reduce its resistance to apoptosis (Guma et al., 2015). In antimalaria studies, CK inhibitors were found to induce parasite death by blocking intraerythrocytic development of *Plasmodium falciparum* (Zimmerman et al., 2013). PfCK has sequence and structure similarities to hCK $\alpha$  which allows human CK inhibitors to inhibit PfCK in low nanomolar concentrations (Zimmerman et al., 2013). In cancer, hCK $\alpha$  was found to be upregulated by different growth factors and oncogene-coding proteins in cancer cells. It participates in tumorigenesis due to its role in biosynthesis of PtdCho (Huang and Freter, 2015). Apart from its involvement in tumor cells, hCK $\alpha$  became an anticancer target because inhibition of CK does not alter PtdCho biosynthesis of non-tumorigenic cells (Lacal, 2015).

The first CK inhibitor found was hemicholinium-3 (HC-3) used in the nervous system. HC-3 blocked choline uptake into presynaptic terminals, preventing the formation of acetylcholine (Gomez et al., 1970). Subsequently in the brain, it was shown to block sodium-dependent high affinity choline uptake, reducing acetylcholine synthesis

(Gardiner, 1961). The off-target effects when HC-3 was used for *in vivo* studies prompted scientist to explore derivatives to improve its specificity on the neuronal choline transporters and acetylcholinesterase (Cannon, 1994). Lacal's group developed a new CK inhibitor based on structures of prior HC-3 derivatives. The synthesized bis-pyridinium compounds gave good potency against purified CK and cancer cells (Campos et al., 2001). One of the compounds developed – MN58b had higher specificity than HC-3 and exhibited growth retardation in several cancer cell lines (Hernández-Alcoceba et al., 1997). Since then, scientists have been working on several aspects of CK inhibitors to improve their antiproliferative properties, potency, and specificity. Changes have been made from using different class of compounds, down to improvisation on the length and structure of linker, distance between quaternary ammoniums, steric hindrance, and delocalization of positive charge (Janardhan et al., 2006, Arlauckas et al., 2016). This study utilizes CK inhibitors to investigate its potential anti-amoebic properties by disrupting *E. histolytica*'s PtdCho biosynthesis.

The synthetic 5-nitroimidazole, metronidazole has been used in treatment of anaerobic bacteria and is the recommended drug in treating amoebiasis for the past 50 years (Löfmark et al., 2010). Metronidazole is effective against anaerobic infections due to sufficient negative redox potential from the presence of electron transport proteins. Once metronidazole enters the cytoplasm via passive diffusion, the electron acceptors have lower redox potential than metronidazole thus donating its electron to the drug. The drug is 'activated' to a nitroso free radical that is cytotoxic. The actual mechanism of action on DNA molecule is unknown but it has been speculated that the activated

metronidazole binds to DNA molecule, inhibiting DNA synthesis and causing DNA damage by oxidation that leads to DNA degradation and cell death (Reysset, 1996).

Although there are no clinically reported metronidazole resistance cases, trophozoites managed to acquire metronidazole resistance *in vitro*. Upcroft's group introduced metronidazole resistance to *E. histolytica* trophozoites after 177 days of selection under microaerophilic conditions (to stimulate actual conditions after tissue invasion) and subsequently the trophozoites were maintained in medium with 10  $\mu$ M of metronidazole (Samarawickrema et al., 1997). Wassmann's group were maintaining trophozoites in medium with 40  $\mu$ M metronidazole (Wassmann et al., 1999). It is difficult to generate metronidazole resistance in *E. histolytica* trophozoites *in vitro* however experiments conducted showed that it is possible for the trophozoites to tolerate constant exposure to metronidazole dosages that are comparable to the recommended dosages currently used in treating amoebiasis.

Investigation on metronidazole resistant *E. histolytica* showed that there was significant increase in superoxide dismutase (SOD) activity and peroxiredoxin meanwhile expression of flavin reductase and ferredoxin 1 decreased. SOD and peroxidase are responsible for oxygen scavenging. The metronidazole resistant mechanism may be explained in the following ways: SOD may be able to detoxify nitro radicals from metronidazole activation. Nitro radicals produced can be removed by SOD that forms hydrogen peroxide. The detoxification of hydrogen peroxide may be catalyzed by peroxiredoxin; flavin reductase may function as a nitroreductase, with the reduced flavin oxidized by metronidazole that leads to formation of nitro radical; microaerophilic conditions causes flavin reductase to reduce oxygen, thus leading to



formation of hydrogen peroxide (Wassmann et al., 1999). Clinical resistance of metronidazole were found in the anaerobic *Giardia lamblia* and *Trichomonas vaginalis* (Upcroft and Upcroft, 2001). Experts have warned against the use of short-term and sub-lethal levels exposure of metronidazole for prophylaxis purposes to prevent induction of drug resistance (Upcroft and Upcroft, 2001).

*EhCK* (XM\_652388.1) is genetically homologous to *hCK $\alpha$ 2* (NM\_001277.2), based on sequence comparison from *E. histolytica* Genome Project (Chang, 2012). *hCK $\alpha$ 2* is a vastly investigated gene due to its association with tumorigenesis and its major role in phosphatidylcholine biosynthesis (Gallego-Ortega et al., 2009, de Molina et al., 2002). Many anti-CK drugs are currently being developed, by targeting the choline and ATP binding pocket of CK $\alpha$  (de la Cueva et al., 2013, Falcon et al., 2013, Hudson et al., 2013). Commercially available known CK inhibitors and compounds with structural similarities to choline/ATP tested in this study were: 2-amino-1-butanol, miltefosine, choline kinase  $\alpha$  inhibitor (CK37), flavopiridol, H-89 dihydrochloride (H-89) hydrate, hemicholinium-3 (HC-3), hexadecyltrimethylammonium bromide (HDTAB), and thiamine hydrochloride.

HC-3 is the prototype for CK inhibitors since 1954 (Long and Schueler, 1954). HC-3 administration has found to have off-target action on acetylcholinesterase and presents high toxicity to cells (Boobis et al., 1975). It is a well-known choline competitive inhibitor that is highly selective towards choline kinase however it has a downside by having high toxicity that stems from its structural similarities to choline (Zech et al., 2016). To reduce its toxicity but preserve its specificity, the structure of HC-3 has been

modified but preserving the symmetrical *bis*-quaternary structure (Hernández-Alcoceba et al., 1997).

Improvisation of HC-3 was done on alternating hydrophobic spacer length between quaternary ammonium groups (Bhattacharyya et al., 1987), the linker moiety, steric hindrance, and the electron donating groups (Janardhan et al., 2006). Other than HC-3 and its derivatives, many other structures such as bis-pyridiniums, bis-quinoliniums, and non-symmetric inhibitors have been explored to increase potency and reduce toxicity (Figure 1.7) (Arlaukas et al., 2016). Many different HC-3 derivatives have been produced such as MN58b (Hernández-Alcoceba et al., 1999) and RSM-932A (Zimmerman et al., 2013, Lacal and Campos, 2014). RSM-932A, also known as TDC-717 has recently completed its Phase I clinical trial successfully (Lacal and Campos, 2014).

N-(3,5-dimethylphenyl)-2-[[5-(4-ethylphenyl)-1H-1,2,4-triazol-3-yl]sulfanyl]acetamide, CK37 was discovered through *in silico* molecular modeling. It was found to inhibit recombinant CK $\alpha$  by targeting the choline binding site. CK37 inhibits endogenous HeLa CK activity at 1  $\mu$ M - 10  $\mu$ M and caused a decrease in phosphocholine and its downstream metabolites (Clem et al., 2011). CK37 dose-dependently suppressed 6 different tumor cell lines (IC<sub>50</sub> between 5  $\mu$ M- 10  $\mu$ M in 48 hours) and selectively exhibit tumor growth suppression in MDA-MB-231 mammary carcinoma cells (IC<sub>50</sub> = 10  $\mu$ M) compared to Human Mammary Epithelial Cells (HMEC) normal epithelial cells (IC<sub>50</sub> = 50  $\mu$ M) (Clem et al., 2011).

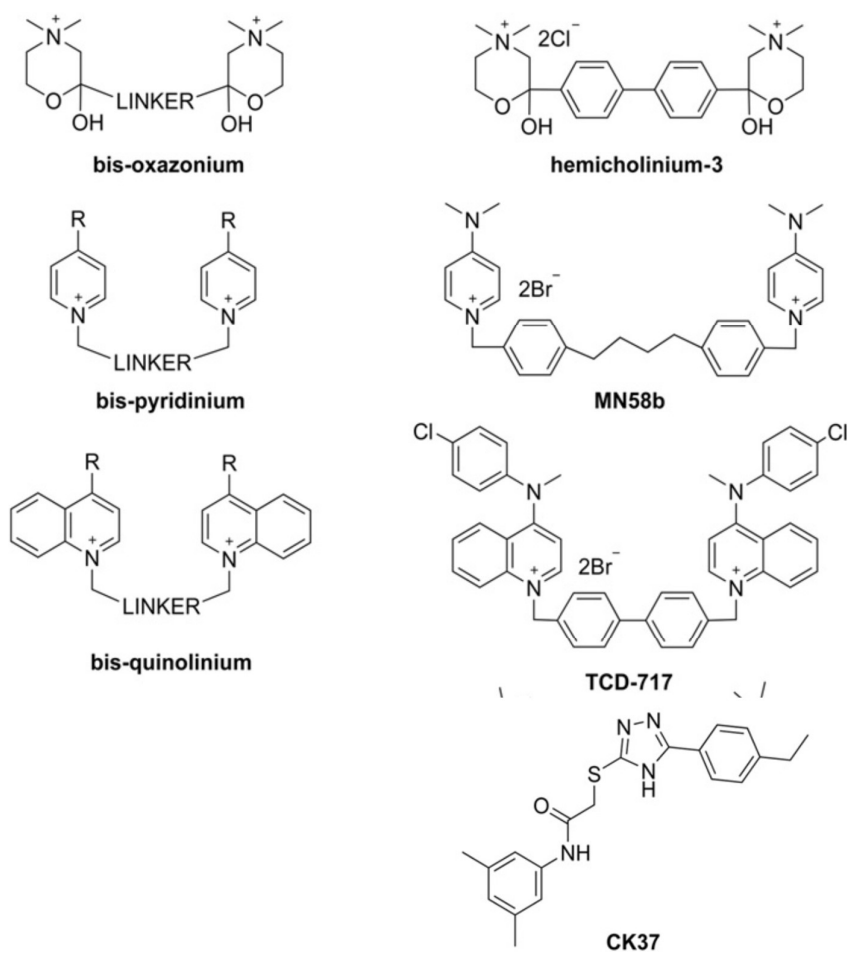


Figure 1.7 CK inhibitors and their structures. CK37 belongs to asymmetry inhibitor that was developed via computational screening approach (Arlauckas et al., 2016).

Flavopiridol (also known as Alvocidib), a flavonoid alkaloid, is a cyclin-dependent kinase inhibitor that acts on CDK9 and CDK 4/6 (Senderowicz, 1999). A combined treatment of SN-38 (metabolite of irinotecan) and flavopiridol reduced phosphocholine:choline concentration in HCT-116 by 67% (Darpolor et al., 2011). Flavopiridol was found to have clinical activity against chronic lymphocytic leukemia (CLL), acute myeloid leukemia (AML), hepatocellular carcinoma, ovarian carcinoma, breast cancer, prostate cancer, and uterine leiomyoma (Wiernik, 2016). It is an ATP competitive inhibitor that promotes apoptosis by preventing cell cycle progression in G2-M or G1-S phase (Baguley and Kerr, 2002). Combination of flavopiridol and other drugs found success in treatment of AML, however its high toxicity, difficult prescription, and emerging of new single-drugs with less toxicity made it unable to advance into phase III trial (Wiernik, 2016).

A potent inhibitor of protein kinase A (PKA), H-89 also inhibits other kinases such as S6KI, ROCKII, K $\beta$  and MAPKAP-K1b (Lochner and Moolman, 2006). H-89 blocks PKA through competitive inhibition of ATP at the ATP site of PKA catalytic subunit (Hidaka et al., 1984). H-89 inhibits CK dose-dependently with an IC<sub>50</sub> = 35  $\mu$ M, with phosphatidylcholine concentration of HeLa cells decreased upon presence of 10  $\mu$ M H-89 (Wieprecht et al., 1994, Gabellieri et al., 2009). Although H-89 could not inhibit PfCK (Choubey et al., 2007) and its binding mechanism on CK is still unknown, it was chosen for this study based on its ability to inhibit hCK.

Better known as vitamin B1 hydrochloride, thiamine HCl is essential for aerobic metabolism, cell growth, transmission of nerve impulses and acetylcholine synthesis (Thomson et al., 1987, Brin, 1962). Thiamine HCl is phosphorylated by thiamine

pyrophosphokinase-1 (TPK1) to form active thiamine pyrophosphate which is a coenzyme for enzymatic activities in fatty acid, amino acid, and carbohydrate metabolism (Nosaka et al., 2001). Alteration to thiamine homeostasis was found to have significant correlation to the increase of cancer cell proliferation, with studies suggest that cancer cells utilize thiamine-dependent enzymes and pathways for proliferation and survival (Zastre et al., 2013, Liu et al., 2010). Thiamine HCl was chosen in this study as one of the inhibitors based on its structural similarities to choline substrate.

HDTAB (also abbreviated as CTAB) is frequently used in plant DNA extraction. A cationic detergent, CTAB forms micelles, a structure similar to plasma membrane, which allows them to incorporate themselves into the membrane phospholipids and disrupt the membrane structure. The quaternary ammonium compound, HDTAB was selected as an inhibitor candidate in this study due to its structural similarities to miltefosine, an anti-proliferative and anti-leishmanial drug (Choubey et al., 2007). Quaternary ammonium derivatives have also been reported to exhibit antitumor activity (Giraud et al., 2002). HDTAB inhibits PfCK in a dose-dependent manner with 60% of PfCK activity inhibited at 100  $\mu$ M by competing with choline at its binding site (Choubey et al., 2007). In the case of tumorigenesis, HDTAB inhibits proliferation of prostate cancer cells besides being identified as a potential candidate in treatment of head and neck cancer (Ito et al., 2009, Wissing et al., 2013). HDTAB targets cancer cells by inhibition of ATP synthase, preventing mitochondrial membrane potential repolarization that leads to caspase activated apoptosis (Ito et al., 2009).

## 1.6 Gene silencing of *E. histolytica*

The phenomenon of double stranded RNA in blocking mRNA was discovered by Andrew Fire and Craig Mello in 1998 and was dubbed as RNA interference (RNAi) (Fire et al., 1998). Since then, RNAi has come a long way to its current use in clinical trials of numerous diseases. RNAi is a catalytic pathway initiated by double stranded RNA (dsRNA). The triggering of this pathway may stem from the naturally occurring dsRNA in the cells, or by introducing dsRNA artificially using certain techniques. Although the mechanism of this pathway differs with organisms, the fundamental principles of RNAi generally starts from introduction of dsRNA. A protein named Dicer, then processes dsRNA into small interfering RNA (siRNA). A single guide strand siRNA was recognized and incorporated into RNA-induced silencing complex (RISC). This siRNA guides RISC complex to complementary mRNA target where the target mRNA is sliced and transcription is halted (Ghildiyal and Zamore, 2009). Ultimately, RNAi causes downregulation of the target gene by degrading its mRNA.

Prior to Andrew Fire and Craig Mello discovery that dsRNA induces highly specific and potent downregulation in *C. elegans*, antisense RNA strand has been used in regulating gene expression (Fire et al., 1998). Antisense RNA was able to regulate gene expression although the downregulation was not as potent as using dsRNA (Nishikura and Murray, 1987). Scientists wanted to use antisense RNA as a therapeutic agent but due to its low potency at low concentrations, there was a raised concern on increasing RNA concentrations as it may lead to cytotoxicity issues (Farrell, 1993). Now dsRNAs, together with other types of siRNAs are used in clinical trials for diseases such as eye diseases, hypercholesterolemia, haemophilia, viruses, and multiple types of cancer (Bobbin and Rossi, 2016).